



ELSEVIER

Available online at [www.sciencedirect.com](http://www.sciencedirect.com)

SCIENCE @ DIRECT®

Nuclear Instruments and Methods in Physics Research B 241 (2005) 341–345

**NIM B**  
Beam Interactions  
with Materials & Atoms

[www.elsevier.com/locate/nimb](http://www.elsevier.com/locate/nimb)

# Damage annealing process in implanted poly-silicon studied by nanocalorimetry: Effects of heating rate and beam flux

R. Karmouch, J.-F. Mercure, Y. Anahory, F. Schiettekatte \*

*Regroupement Québécois sur les Matériaux de Pointe (RQMP), Département de Physique, Université de Montréal, C.P. 6128 succ. centre-ville, Montréal, Qué., Canada H3C 3J7*

Available online 18 August 2005

## Abstract

Nanocalorimetry of ion-implanted damage annealing in polycrystalline Si is presented. Si was implanted at 30 keV. Temperature scans were performed between room temperature and 350 °C at heating rates between 48 and 144 kK/s for a fluence of  $1 \times 10^{13}$  Si/cm<sup>2</sup>, and between room temperature and 540 °C at beam fluxes of 11 and 44 nA/cm<sup>2</sup> with a fluence of  $2 \times 10^{13}$  Si/cm<sup>2</sup>. The heat release shows no features, but rather a broad increase with temperature which is characteristic of a series of processes continuously distributed in terms of activation energy. Higher heating rates shift the signal towards higher temperatures and decrease its amplitude, which is typical for thermally activated processes. Lower beam flux implants translate into smaller heat release. This is partly attributed to shorter implantation times at higher fluxes, which leave less time for dynamic annealing, but could also be due to the higher impact rate in the environment of previously generated disordered zones. Such impact generates damage that may stabilize disordered zones, which would have enough time to undergo dynamic annealing at lower fluxes.

© 2005 Elsevier B.V. All rights reserved.

PACS: 61.72.Cc; 07.20.Fw

Keywords: Nanocalorimetry; Ion implantation; Damage annealing; Heat rate; Beam flux

## 1. Introduction

Semiconductor doping by ion implantation is facing many challenges as the technology evolves towards ultra-shallow junctions and transistor half-pitch well below 100 nm [1]. By generating defects in the lattice, implantation strongly influences the way dopants diffuse and are activated. It was

\* Corresponding author. Tel.: +1 514 343 6049; fax: +1 514 343 7357.

E-mail address: [francois.schiettekatte@umontreal.ca](mailto:francois.schiettekatte@umontreal.ca) (F. Schiettekatte).

evidenced that point defect go through a clustering phase before forming {3 1 1} rod-like defects around 700 °C [2]. Their coarsening is responsible for the transient enhanced diffusion [3].

Recently, our group introduced nanocalorimetry as a way to investigate from the thermal point of view the kinetics of damage annealing in silicon implanted at low energy [4,5]. This technique operates on similar principles as conventional differential scanning calorimetry (DSC), but fast heating rates ( $10^4$ – $10^6$  K/s) and low thermal losses make possible the observation of thermal processes in thin films or at surface, involving energies of the order of the nJ [6]. Considering the type of information it provides in terms of activation energies and amount of heat released by low energy implantation defects, nanocalorimetry can be extremely useful in elucidating the mechanisms underlying damage annealing. In implanted polycrystalline silicon (poly-Si), it was shown recently that the amount of heat released as a function of temperature has the same shape from very low to high fluences [5]. This implies that the underlying processes are the same, as if each impacting ion readily produced damage structures similar to what is found in heavily damaged Si. In this paper, we report on nanocalorimetry experiments, where the heat released by damage annealing following self-implantation of poly-Si is investigated for different heating rates and beam currents.

## 2. Nanocalorimetry experiments

Our nanocalorimeters consist of a low stress  $\text{Si}_3\text{N}_x$  membrane 150 nm thick on the surface of which is deposited a Pt strip (25 nm thick, 0.5 mm in width, 7.4 mm in length). This strip serves both as a heater and a thermometer, through a resistance measurement. For our implantation experiments, a 140 nm amorphous Si layer was deposited by plasma sputtering on the opposite side of the membrane, in line with the Pt heater. The membrane ensures a good thermal conduction between the sample and the heater, while it isolates them electrically. Prior to the implantations, the nanocalorimeters were annealed at 900 °C during

100 s in a  $\text{N}_2$  atmosphere to form a poly-Si layer with crystallites of  $\sim 75$  nm.

Nanocalorimetry measurements are initiated by supplying a current pulse of 8 ms to the Pt heater, thus raising the temperature of the system by Joule heating. Here, the current pulses varied from  $\sim 35$  mA to  $\sim 57$  mA, providing heating rates between 48 and 145 kK/s. For slower scans, subsequent higher heating rate scans were performed in order to ensure proper annealing at more than 700 °C. The current and voltage were monitored in real time during the pulse, so the heat supplied to the system ( $P = VI$ ) was obtained. The temperature during the scan was determined using a calibration of the Pt strip resistance versus temperature established beforehand. However, the implanted nanocalorimeter overheated during the fastest scans, which came the last, causing its resistance to change by 4%. This resulted in an error of 10 °C on the temperature scale for this scanning rate. The measurements were achieved in differential mode using two nanocalorimeters placed side-by-side in the implantation chamber, one of them being implanted (imp) in order to induce damage, while the other served as reference (ref) and remain unimplanted. A detailed description of the method used to extract the heat capacity of a deposited layer, including the subtraction of baselines to account for the fact that the implanted and reference calorimeters are not identical, and to correct for thermal losses, can be found in [7],[8]. Here, poly-Si is deposited on both nanocalorimeters, so heat capacity does not nominally contribute any net signal; only damage annealing does. Any difference in heat capacity between the implanted and reference nanocalorimeters is subtracted by carrying out baseline measurements. Roughly, the heat rate, i.e. the amount of heat transferred to a process per unit degrees, is given by

$$q(T) = (VI/v)_{\text{imp}} - (VI/v)_{\text{ref}} \quad (1)$$

where  $v$  is the temperature scanning rate. The effect of damage annealing, by releasing heat to the implanted nanocalorimeter, is to increase slightly its heating rate. A released heat thus corresponds to a negative value of  $q(T)$ . The results presented here show amounts of heat released, thus  $-q(T)$ .

Low-energy Si<sup>-</sup> implantations were performed by extracting negatively charged ions from a sputter source biased at the desired voltage, without net acceleration inside a Tandemron accelerator. Implantations were carried out at room temperature (RT) at an energy of 30 keV. The fluence was set to  $1 \times 10^{13}$  Si/cm<sup>2</sup> for experiments at different heating rates, and  $2 \times 10^{13}$  Si/cm<sup>2</sup> for those at different beam fluxes. According to SRIM 2003 simulations [9], no ions reached the Si<sub>3</sub>N<sub>x</sub> membrane, all being stopped within the poly-Si layer. Each implantation was followed by 10 scans. During each scan the nanocalimeters heated up to 700 °C or more, which should be sufficient to anneal any remaining damage. No measurable amount of heat was released after the first scan, the signals of scans from 2 to 10 falling back exactly on the baseline obtained prior to the implantations [8].

### 3. Heating rate

As seen from Fig. 1, heat released by damage annealing shows a broad, featureless temperature dependence that can be associated to a continuous spectrum of thermally activated processes. This underlines how the annealing of low-energy ion-

implanted Si occurs through a wide spectrum of steps [5]. According to molecular dynamics simulations, heavy ion implantation generates so-called amorphous pockets [10] or defect clusters [11] in which the majority of the surviving induced defects are stored. These highly disordered zones undergo annealing through sudden partial recrystallization steps. Their lifetime generally increases with size, but what triggers such recrystallization highly depends on the details of the disordered-crystalline interface, so no specific or unique activation energy can be established [12]. As most displaced atoms are found in these zones, we consider that their annealing dominates the heat release. Consequently, the results discussion presented here is based on this interpretation.

Changing parameters such as the heating rate is useful to extract information like the order of the kinetics of the processes going on. From Fig. 1, one can see that as the heating rate increases, the heat rate curves shift towards high temperature and decrease in amplitude, as it is usually the case for thermally activated processes: compared to slower scans, faster scans leave less time for the processes to be activated, thus for damage to anneal and to release heat.

We then compared the heat rate curves to a model that considers processes continuously distributed in terms of activation energy. Let  $C(E, t)$  be the density of unactivated processes after a time  $t$  per unit activation energy, initially at a constant value  $C_0$ . Each process releases a heat  $H_0$  upon activation. Considering first order kinetics, the number of processes of activation energy  $E$  occurring at temperature  $T(t)$  during time  $dt$  is proportional to the number of remaining unactivated processes. We thus have

$$dC(E, t) = f_0 C(E, t) e^{-E/kT(t)} dt, \quad (2)$$

where  $f_0$  is the trial frequency ( $10^{13}$  Hz). The heat rate then becomes

$$q(T(t)) = \nu H_0 \int \frac{dC(E, t)}{dt} dE, \quad (3)$$

that is, the sum of the number of processes that occurred at any activation energy  $E$  during  $dt$ , multiplied by the amount of heat they released and the heating rate.

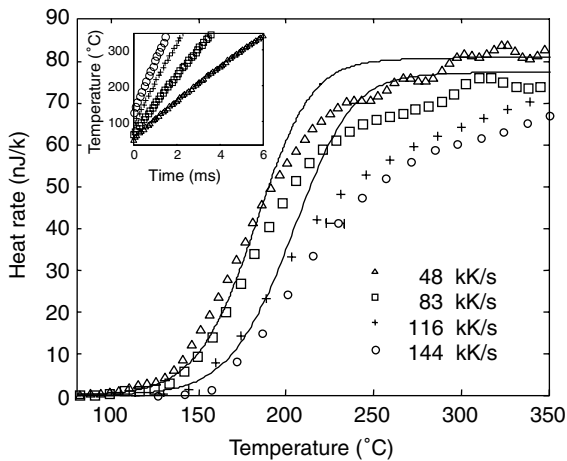


Fig. 1. Heat released by poly-Si implanted with 30 keV Si<sup>-</sup> at  $1 \times 10^{13}$  Si/cm<sup>2</sup> for different heating rates. Solid lines are the heat release calculated from Eq. (3) for heating rates of 48 kK/s (left) and 144 kK/s (right). The inset indicates the temperature as a function of time for each measurement.

In Fig. 1, solid lines illustrate  $q(T)$  calculated for scans at 48 and 144 kK/s. The calculations include an initial RT annealing to account for the fact that nanocalorimetry scans are carried out  $\sim 30$  s after the implant. While the model offers limited agreement with the data, the initial phase of the heat release is relatively well reproduced, as is the shift toward higher temperature with increasing scanning rate.

In the context of highly disordered zones, first-order kinetics means that number of recrystallization events simply depends on the number of available, unactivated processes at a given energy. The continuous distribution in terms of activation energy reflects the fact that each crystallization event primarily depends on the detailed structure and stability of the disordered-crystalline interface of each zone: the wide spectrum of configurations translates into a continuous spectrum of activation energies. We also considered a second-order kinetics model, but it does not reproduce the data as well, although it features similar temperature shift and amplitude decrease with temperature. Considering the limited agreement with data, such model is probably too simple to account for all effects occurring in the sample, which may include processes at several different kinetic orders.

#### 4. Beam flux

We now review results obtained by nanocalorimetry after implantation at two different beam fluxes: 11 and 44 nA/cm<sup>2</sup>. This time a fluence of  $2 \times 10^{13}$  Si<sup>-</sup>/cm<sup>2</sup> was accumulated. Three implantations were carried out: we started with the higher beam current, followed by an implantation at the lower current, and then again at the higher current. The results are presented in Fig. 2. The same signal is obtained for both high current implantations. This demonstrates that measurements are not altered by implant history. Temperature scans reaching 700 °C are thus sufficient to anneal the material so following damage generation is not affected, within the sensitivity limit.

It is also seen that damage releases remarkably more heat after high beam current implantations,

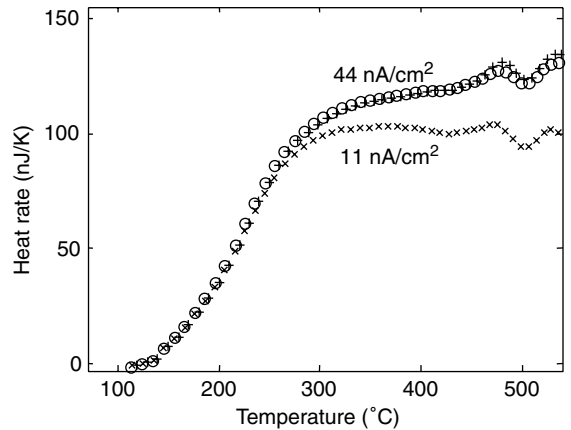


Fig. 2. Heat released by poly-Si implanted with 30 keV Si<sup>-</sup> at a fluence of  $2 \times 10^{13}$  Si<sup>-</sup>/cm<sup>2</sup> for different beam fluxes in the following order: 44 nA/cm<sup>2</sup> (+), 11 nA/cm<sup>2</sup> (x), and 44 nA/cm<sup>2</sup> (o).

suggesting that damage undergoes more dynamics annealing at comparatively low beam current ion implantation, simply because the implantation time is longer. As a result, fewer processes are available for annealing during the scan, releasing less heat. But another effect may come into play. Some highly disordered zones may have undergone recrystallization before another ion impacts nearby during an implant at low current. But at higher current, more frequent impacts may stabilize such structures by producing displacements in the same region, displacements that may have otherwise quickly anneal out at RT. The rationales behind this effect relate to the characteristic lifetime and size of disordered zones. For 30 keV Si, the radius of a cascade is of the order of  $r = 10$  nm. Considering a cylinder of radius  $r$ , an ion impacts about every second on average at a beam flux of 44 nA/cm<sup>2</sup>, while one impact about every 5 s at 11 nA/cm<sup>2</sup>. The characteristic lifetime of the disordered zones involved in this effect should thus be of the order of 1 s. Again, lifetimes are dependent of disordered zone size [10], although it differs considerably for zones with similar size [12]. As a wide spectrum of lifetimes is present in such sample, perhaps extending from ns to years, we expect this effect to extend over orders of magnitude in terms of beam flux.

## 5. Summary

In conclusion, we showed the ability of nanocalorimetry to investigate the kinetics of damage annealing following low-energy ion implantation. The heat release observed is characteristic of a series of thermally activated processes continuously distributed in terms of activation energy. This is also evidenced by the fact that faster heating rates shift the heat release toward higher temperature and decrease its amplitude. It appears that dynamic damage annealing is more efficient at lower beam current, since the amount of heat release during the scan is smaller. This may be attributed in part to the shorter implantation time at higher beam flux, leaving less time for dynamic annealing, but it could also be attributed to the higher event rate in the environment of previously generated disordered zones that are stabilized by such events before they have enough time to anneal.

## Acknowledgements

The authors are grateful to S. Roorda and M. Chicoine (Université de Montréal), and L.H. Allen and M.Yu. Efremov (UIUC) for fruitful discussions. Thanks also go to Y.Q. Wang for TEM, L. Godbout, R. Gosselin for their technical assistance with the accelerator operation, and M. Skvarla and P. Infante of the Cornell Nanofabrication Facility, as well as M.-H. Bernier and S. Bah of the École Polytechnique de Montréal for

their assistance with nanocalorimeters fabrication. This work benefited from the financial support of NanoQuébec, the Fonds Québécois de Recherche sur la Nature et les Technologies and the Natural Science and Engineering Research Council of Canada.

## References

- [1] International Technology Roadmap for Semiconductors, Edition 2003.
- [2] N.E.B. Cowern, G. Mannino, P.A. Stolk, F. Roozeboom, H.G.A. Huizing, J.G.M. van Berkum, A. Claverie, F. Cristiano, M. Jaraiz, *Phys. Rev. Lett.* 82 (1999) 4460.
- [3] B. Colombeau, N.E.B. Cowern, F. Cristiano, P. Calvo, N. Cherkashin, Y. Lamrani, A. Claverie, *Appl. Phys. Lett.* 83 (2003) 1953.
- [4] J.-F. Mercure, R. Karmouch, S. Roorda, F. Schiettekatte, Y. Anahory, *Physica B* 340–342 (2003) 622.
- [5] R. Karmouch, J.-F. Mercure, Y. Anahory, F. Schiettekatte, *Appl. Phys. Lett.* 86 (2005) 031912.
- [6] M.Y. Efremov, F. Schiettekatte, M. Zhang, E.A. Olson, A.T. Kwan, R.S. Berry, L.H. Allen, *Phys. Rev. Lett.* 85 (2000) 3560.
- [7] M.Yu. Efremov, E.A. Olson, M. Zhang, S.L. Lai, F. Schiettekatte, Z.S. Zhang, L.H. Allen, *Thermochim. Acta* 412 (2004) 13.
- [8] R. Karmouch, J.-F. Mercure, F. Schiettekatte, *Thermochim. Acta* 432 (2005) 186.
- [9] J.F. Ziegler, J.P. Biersack, U. Littmark, *The Stopping and Range of Ions in Solids*, Pergamon Press, New York, 1985.
- [10] M.-J. Caturla, T. Diaz de la Rubia, L.A. Marques, G.H. Gilmer, *Phys. Rev. B* 54 (1996) 16683.
- [11] K. Nordlund, M. Ghaly, R.S. Averback, M. Caturla, T. Diaz de la Rubia, J. Tarus, *Phys. Rev. B* 57 (1998) 7556.
- [12] S.E. Donnelly, R.C. Birtcher, V.M. Vishnyakov, G. Carter, *Appl. Phys. Lett.* 82 (2003) 1860.